Dynamics and molecular interactions of linker of nucleoskeleton and cytoskeleton (LINC) complex proteins

Cecilia Östlund[1,2], Eric S. Folker[2], Jason C. Choi[1,2], Edgar R. Gomes[2,*], Gregg G. Gundersen[2] and Howard J. Worman[1,2,‡]

[1]Department of Medicine, and [2]Department of Pathology and Cell Biology, College of Physicians and Surgeons, Columbia University, New York, New York 10032, USA

*Present address: UMB S 787 INSERM, Université Pierre et Marie Curie Paris VI, Paris 75634, France
‡Author for correspondence (hjw14@columbia.edu)

Accepted 10 September 2009
Journal of Cell Science 122, 4099-4108 Published by The Company of Biologists 2009
doi:10.1242/jcs.057075

Summary

The linker of nucleoskeleton and cytoskeleton (LINC) complex is situated in the nuclear envelope and forms a connection between the lamina and cytoskeletal elements. Sun1, Sun2 and nesprin-2 are important components of the LINC complex. We expressed these proteins fused to green fluorescent protein in embryonic fibroblasts and studied their diffusional mobilities using fluorescence recovery after photobleaching. We show that they all are more mobile in embryonic fibroblasts from mice lacking A-type lamins than in cells from wild-type mice. Knockdown of Sun2 also increased the mobility of a short, chimeric form of nesprin-2 giant (mini-nesprin-2G), whereas the lack of emerin did not affect the mobility of Sun1, Sun2 or mini-nesprin-2G. Fluorescence resonance energy transfer experiments showed Sun1 to be more closely associated with lamin A than is Sun2. Sun1 and Sun2 had similar affinity for the nesprin-2 KASH domain in plasmon surface resonance (Biacore) experiments. This affinity was ten times higher than that previously reported between nesprin-2 and actin. Deletion of the actin-binding domain had no effect on mini-nesprin-2G mobility. Our data support a model in which A-type lamins and Sun2 anchor nesprin-2 in the outer nuclear membrane, whereas emerin, Sun1 and actin are dispensable for this anchoring.

Key words: LINC complex, Sun1, Sun2, Nesprin, Nuclear envelope, Lamin, Emerin

Introduction

Several proteins specific to the inner and outer nuclear membranes have been identified as components of the LINC (linker of nucleoskeleton and cytoskeleton) complex (Crisp et al., 2006; Tzur et al., 2006; Worman and Gundersen, 2006). This complex forms a connection between the lamina and the cytoskeleton and has been shown to be important for nuclear positioning and nuclear migration (Starr, 2009; Tzur et al., 2006; Worman and Gundersen, 2006). The LINC complex is primarily composed of Suns and nesprins (also called synes), but other nuclear envelope proteins, such as emerin, might also be components (Crisp et al., 2006; Libotte et al., 2005). Mutations in *SYNE1*, which encodes nesprin-1, lead to autosomal recessive cerebellar ataxia (Gros-Louis et al., 2007). Mutations or polymorphisms in *SYNE1* and *SYNE2*, which encodes nesprin-2, have been identified in probands with Emery-Dreifuss muscular dystrophy or similar phenotypes (Zhang et al., 2007a). Abnormalities in the structure and function of the LINC complex might also contribute to the pathogenesis of diseases caused by mutations in genes encoding other nuclear envelope proteins (Worman and Gundersen, 2006).

Nesprins have multiple spectrin repeats in their nucleo-cytoplasmic N-terminal regions, followed by a conserved KASH domain, consisting of a transmembrane segment and approximately 30 lumenal amino acids (Starr and Fischer, 2005). In their N-terminus, larger nesprin isoforms have paired actin-binding calponin homology (CH) domains (Padmakumar et al., 2004; Tzur et al., 2006; Zhen et al., 2002). There are four known mammalian nesprin genes: *SYNE1* and *SYNE2* each encode several isoforms of varying molecular masses, some being very large, for example 796 kDa for nesprin-2 giant. Nesprin-3 and nesprin-4 are lower molecular mass proteins, encoded by separate genes, which bind to plectin and kinesin-1, respectively, but lack the actin-binding domains (Roux et al., 2009; Wilhelmsen et al., 2005). Mammalian nesprins are variably expressed in many tissues (Apel et al., 2000; Zhang et al., 2001; Zhen et al., 2002).

Keratinocytes deficient in nesprin-2 giant have abnormal size and morphology, and fibroblasts from *Syne2* knockout mice (with the exons encoding the CH domain deleted) have deficiencies in migration and cell polarity (Lüke et al., 2008). Disruption of the *Syne1* gene in mice by deletion of the KASH domain affects myonuclear anchorage, and motor neuron innervation and *Syne1*/*Syne2* double KASH domain knockout mice die shortly after birth (Zhang et al., 2007b). It is not clear to what extent different nesprin isoforms are localized in the inner and the outer nuclear membrane. It has been proposed that larger isoforms are excluded from the inner nuclear membrane due to their size, whereas smaller isoforms might be present in both the inner and outer nuclear membranes (Worman and Gundersen, 2006; Zhang et al., 2005). However, nesprin-2 isoforms containing the actin-binding domain have also been reported in the inner nuclear membrane (Libotte et al., 2005). There are also reports of nesprin isoforms targeting to other nuclear and cytoplasmic locations, such as sarcomeres (Warren et al., 2005; Zhang et al., 2002).

Sun1 and Sun2 are type II integral membrane proteins of the inner nuclear membrane. They contain a nucleoplasmic N-terminal domain followed by a transmembrane-spanning region, a luminal

domain with two coiled-coil domains and a homologous, conserved region called the SUN domain (Hodzic et al., 2004; Padmakumar et al., 2005). The sequence similarities between Sun1 and Sun2 are limited to the SUN domain (Crisp et al., 2006; Hodzic et al., 2004; Liu et al., 2007; Wang et al., 2006). Both Sun1 and Sun2 are widely expressed in a variety of tissues (Wang et al., 2006). Two other mammalian proteins, Sun3 and Spag4, also have a Sun-protein structure; the expression levels and tissue distributions of these proteins are much more restricted (Stewart-Hutchinson et al., 2008). *Sun1* knockout mice develop normally but are sterile, with telomere attachment abnormalities leading to meiosis defects (Ding et al., 2007). The mice also exhibit a decrease in number of synaptic nuclei (Lei et al., 2009). Suns have also been implicated in nuclear positioning, centromere localization and apoptosis (Tzur et al., 2006), but their specific functions, as well as potential redundancies, remain poorly understood.

The mechanism for localization and retention of the LINC complex proteins to the nuclear envelope is not well understood and available data are sometimes conflicting. Lamins have been shown to be essential for the proper localization and retention of emerin and MAN1 to the inner nuclear membrane (Gruenbaum et al., 2002; Liu et al., 2003; Östlund et al., 2006; Sullivan et al., 1999; Vaughan et al., 2001) and are possibly involved in the localization and retention of the Suns. The N-terminal domains of Sun1 and Sun2 interact with lamin A, and weakly with lamins B1 and C (Crisp et al., 2006; Haque et al., 2006). Both Sun1 and Sun2 are resistant to detergent, urea and high-salt extractions, indicating that they are integral membrane proteins with a tight interaction with the lamina (Haque et al., 2006; Hodzic et al., 2004; Tzur et al., 2006). However, Sun1 is properly localized in *Lmna*-null mouse embryonic fibroblasts (MEFs) and HeLa cells with A-type lamins depleted by siRNA, indicating that Sun1 localization is not dependent on A-type lamins in mammalian cells (Crisp et al., 2006; Haque et al., 2006; Hasan et al., 2006; Padmakumar et al., 2005). Analysis using fluorescence recovery after photobleaching (FRAP) in HeLa cells also showed Sun1 fused to green fluorescent protein (GFP) to be as immobile in cells depleted of lamin A, B1 or C as in wild-type cells (Hasan et al., 2006). Sun2 is partially displaced to the cytoplasmic membranes in *Lmna*-null MEFs but this displacement is not rescued by lamin A and/or C expression in these cells, indicating that additional factors are involved in Sun2 localization (Crisp et al., 2006). Sun1 is highly immobile in the nuclear membrane, with both its nucleoplasmic and the coil-coiled domains contributing to its immobilization (Lu et al., 2008). The luminal region is not necessary for Sun1 and Sun2 nuclear envelope localization (Crisp et al., 2006; Hasan et al., 2006; Hodzic et al., 2004; Lu et al., 2008; Wang et al., 2006). Overexpression of Sun1 displaces Sun2 but the converse is not true, indicating that proper Sun1 localization depends on additional binding partners (Crisp et al., 2006). Sun1, but not Sun2, has been shown to associate with nuclear pore complexes, suggesting that nuclear pore complex proteins are candidate partners (Liu et al., 2007).

Several studies have shown lamins to be involved in the nuclear envelope localization of nesprins. In SW13 cells, which lack lamin A and have reduced levels of lamin C, as well as in fibroblasts from *Lmna*-null mice and from an individual with a homozygous nonsense *LMNA* Y259X mutation, nesprin isoforms are mislocalized to the bulk endoplasmic reticulum, similar to emerin (Libotte et al., 2005; Muchir et al., 2003; Zhang et al., 2005). Nesprin-2 localization is also altered in fibroblasts carrying a mutation in *LMNA* (S143F) causing myopathy and progeria (Kandert et al., 2007). Nesprins localized in the inner nuclear membrane interact with emerin and A-type lamins (Libotte et al., 2005; Mislow et al., 2002a; Mislow et al., 2002b; Zhang et al., 2005). However, nesprin isoforms situated in the outer nuclear membrane cannot bind directly to lamins because they are in different cellular compartments. Also, the KASH domain is essential for localization of nesprins to the nuclear envelope (Libotte et al., 2005; Padmakumar et al., 2005; Wilhemsen et al., 2005; Zhang et al., 2001; Zhen et al., 2002), but this region does not interact with the lamins. These results imply that nesprins are retained in the nuclear envelope by an indirect interaction with lamins. Suns could mediate such an interaction because Sun1 and Sun2 have been shown to interact with the KASH domains from nesprins 1, 2 and 3 (Crisp et al., 2006; Padmakumar et al., 2005; Stewart-Hutchinson et al., 2008) and because *Sun1/Sun2* double-knockout mice show a disruption of the localization of nesprin-1 to the nuclear envelope in muscle cells (Lei et al., 2009). The inconsistent and conflicting data summarized above warrants a systemic analysis of the protein dynamics and interactions of the LINC complex. We therefore used FRAP to look for specific alterations in LINC complex protein mobility induced by changes in the interactions between lamins, emerin, Suns and nesprins. We also obtained data on the relative affinities of binding of Sun1 and Sun2 to lamin A and the KASH domain of nesprins to elucidate putative differences in function between the Sun proteins.

Results

Localization and dynamics of GFP-tagged LINC complex proteins

To study the dynamics of Sun1, Sun2 and nesprin-2 giant, we expressed them in MEFs as GFP-fusion proteins (Fig. 1A). As nesprin-2 giant contains 6874 amino acids, making cloning a full-length cDNA difficult, we used a shorter, artificial construct (mini-nesprin-2G), not representing a known nesprin-2 variant. The construct contains the N-terminal, actin-binding CH region and two adjacent spectrin repeats fused to the C-terminal KASH domain and the two spectrin repeats preceding it (amino acids 3-485 and 6525-6874, respectively). Although this construct lacks spectrin-repeats of nesprin-2 giant, it is predicted to bind both actin and Suns and can rescue actin-dependent nuclear movement defects in cells depleted of nesprin-2 giant (Luxton, G. W., E.R.G., E.S.F., Vintinner, E. and G.G.G., unpublished results). All three GFP-fusion proteins were localized to the nuclear rim in wild-type MEFs with relatively low expression levels (Fig. 1B, upper row). Similarly to wild-type MEFs, the GFP-fusion proteins were localized to the nuclear rim in MEFs lacking A-type lamins (Sullivan et al., 1999). However, this was often in combination with partial localization to the cytoplasm, especially in the case of GFP-Sun1 and GFP-mini-nesprin-2G (Fig. 1B, bottom row). To assess whether the GFP-fusion proteins were localized to the inner or the outer nuclear membrane, immunofluorescence microscopy was performed using cells treated with digitonin (Fig. 1C), which permeabilizes the plasma membrane but leaves the nuclear membranes intact (Adam et al., 1992). Antibodies against GFP can access proteins in the outer nuclear membrane, but not in the inner nuclear membrane, whereas GFP fluorescence from either compartment can be seen. In transfected cells expressing GFP-mini-nesprin-2G, there was a clear nuclear rim signal both with GFP fluorescence (left panels) and anti-GFP antibodies recognized by rhodamine-labeled secondary antibodies (middle panels). In cells transfected with constructs expressing GFP-Sun1 or GFP-Sun2, only GFP fluorescence was seen at the nuclear envelope, whereas staining with anti-GFP antibodies only showed

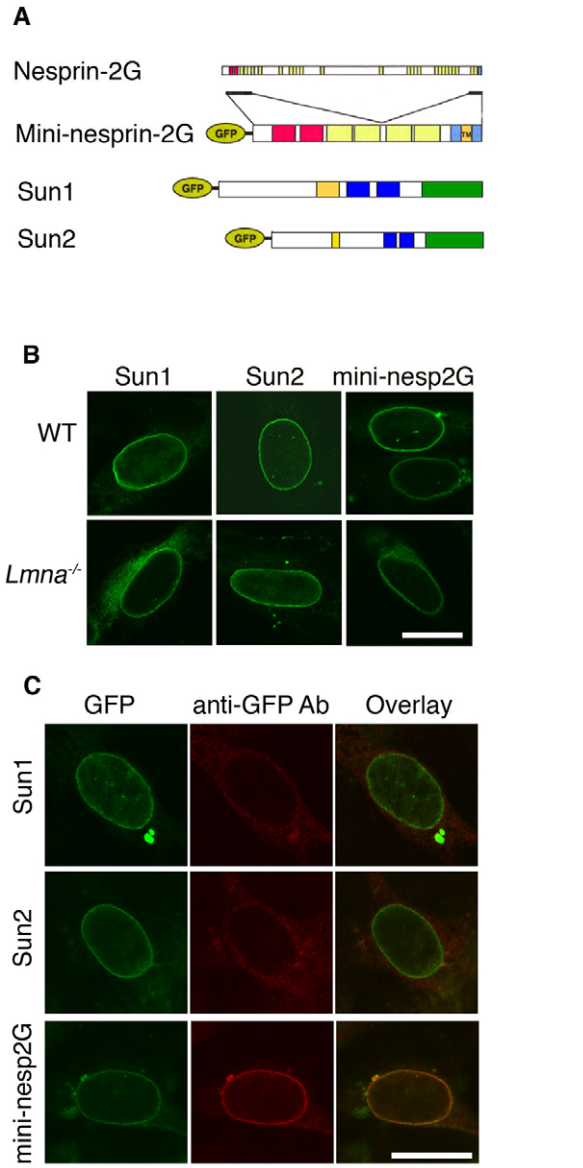

Fig. 1. GFP-tagged Sun1 and Sun2 localize to the inner nuclear membrane whereas GFP-tagged mini-nesprin-2G localizes to the outer nuclear membrane. (A) Schematic depiction of GFP-mini-nesprin-2G, GFP-Sun1 and GFP-Sun2. Diagram of nesprin-2 giant (Nesprin-2G) is shown above GFP-mini-nesprin-2G to indicate portions of the full-length protein that it contains. Red boxes denote CH domain; yellow boxes, spectrin repeats; light blue boxes, the KASH domain; orange boxes, transmembrane-spanning segments; dark blue boxes, coiled-coil domains; and green boxes, SUN domains. (B) GFP-Sun1, GFP-Sun2 and GFP-mini-nesprin-2G localize to the nuclear envelope in transiently transfected wild-type (WT, upper panels) or *Lmna*$^{-/-}$ (lower panels) MEFs. In *Lmna*$^{-/-}$ MEFs, the proteins are also partially found in the cytoplasmic compartment. Panels show laser scanning confocal microscopy images of representative MEFs transiently transfected with plasmids encoding GFP-Sun1, GFP-Sun2 or GFP-mini-nesprin-2G. (C) Wild-type MEFs were transfected as in B, fixed and treated with 40 μg/ml digitonin. Left panels show GFP fluorescence and middle panels staining by anti-GFP antibodies recognized by rhodamine-labeled secondary antibodies. In cells transfected with GFP-Sun1 or GFP-Sun2, only GFP fluorescence was seen at the nuclear envelope, whereas staining with anti-GFP antibodies only shows cytoplasmic background staining. Scale bars: 10 μm.

cytoplasmic background staining. These results confirmed that GFP-Sun1 and GFP-Sun2 were localized primarily in the inner nuclear membrane, like their endogenous counterparts, whereas GFP-mini-nesprin-2G localized to the outer nuclear membrane. That some GFP-mini-nesprin-2G also might be localized in the inner nuclear membrane cannot, however, be ruled out in this type of experiment.

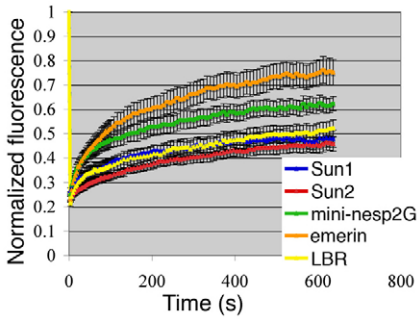

Fig. 2. The mobility of emerin-GFP and GFP-mini-nesprin-2G in the nuclear envelope is higher than the mobility of GFP-Sun1, GFP-Sun2 and LBR-GFP in wild-type MEFs. Quantitative experiments showing normalized fluorescence recovery after photobleaching regions of the nuclear envelope in cells transiently transfected with cDNA encoding GFP-labeled protein, as indicated by the color-coded lines. Normalized fluorescence of 1 is the level before bleaching. The fluorescence intensity in the bleached region was measured, normalized and expressed as relative recovery (see Materials and Methods). Error bars indicate s.e.m., $n \geq 12$.

To investigate the diffusional mobility of GFP-Sun1, GFP-Sun2 and GFP-mini-nesprin-2G, we performed FRAP. GFP-tagged proteins in an area of the nuclear envelope of transiently transfected MEFs were irreversibly bleached using an argon laser at high power. The fluorescence recovery in the bleached area, corresponding to the influx of unbleached molecules from other areas, was then monitored. As controls, we used GFP-fusion proteins of emerin and LBR (lamin B receptor), which we had previously studied using FRAP (Ellenberg et al., 1997; Östlund et al., 1999; Östlund et al., 2006). GFP-Sun1 and GFP-Sun2 were relatively immobile, with recovery dynamics similar to that of LBR-GFP. Similar results have been reported previously for Sun1 (Hasan et al., 2006; Liu et al., 2007; Lu et al., 2008). GFP-mini-nesprin-2G recovered more rapidly than the Suns, although not as completely or rapidly as emerin (Fig. 2). Initial recovery rates were expressed as the $t_{1/2}$ (see Materials and Methods), which was 148.9±18.7 seconds for GFP-mini-nesprin-2G and 107.7±14.2 seconds for emerin-GFP. Due to the low recovery of GFP-Suns and LBR-GFP, calculation of $t_{1/2}$ was not meaningful for these proteins. These data show that the GFP-fusion proteins localize to the nuclear envelope, where they have a relatively low diffusional mobility.

Proteins of the LINC complex are more mobile in cells lacking A-type lamins than in cells lacking emerin or wild-type cells

As Sun1, Sun2 and some short isoforms of nesprin-2 have been shown to interact with A-type lamins, we compared the mobility of GFP-Sun1, GFP-Sun2 and GFP-mini-nesprin-2G in cells lacking A-type lamins to their mobility in wild-type cells. Fluorescence of emerin-GFP was previously shown to recover more rapidly and to a higher degree after bleaching in MEFs lacking A-type lamins than in wild-type cells, whereas the recovery of fluorescence of LBR-GFP was the same in the two cell types (Östlund et al., 2006). GFP-Sun1, GFP-Sun2 and GFP-mini-nesprin-2G all recovered more quickly in MEFs lacking A-type lamins than in wild-type MEFs (Fig. 3A-C). When exogenous RFP-lamin A was co-expressed with GFP-Sun1 in *Lmna*$^{-/-}$ MEFs, GFP-Sun1 showed fluorescence

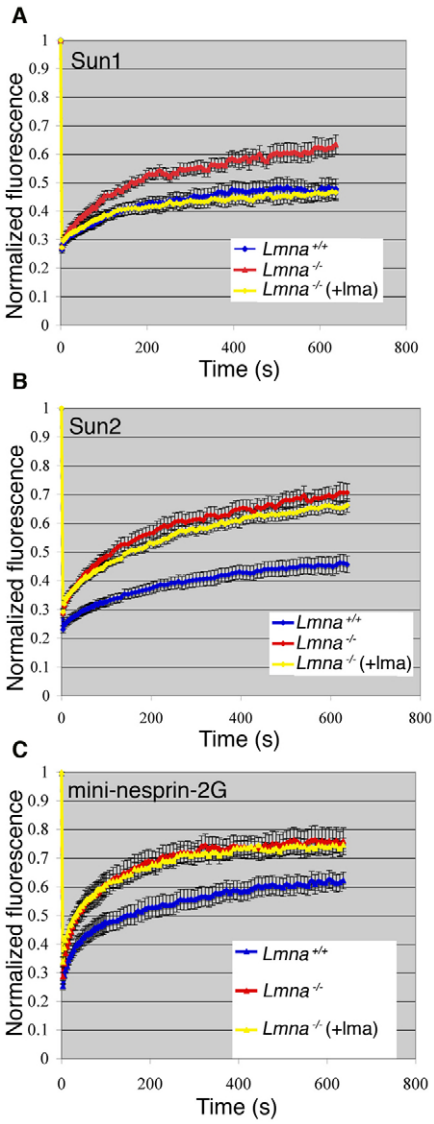

Fig. 3. Proteins of the LINC complex are more mobile in MEFs lacking A-type lamins than in wild-type MEFs. Quantitative experiments, as described in Fig. 2, showing normalized fluorescence recovery after photobleaching of (A) GFP-Sun1, (B) GFP-Sun2 and (C) GFP-mini-nesprin-2G in wild-type MEFs (*Lmna*$^{+/+}$), *Lmna*$^{-/-}$ MEFs (*Lmna*$^{-/-}$) or *Lmna*$^{-/-}$ MEFs co-transfected with cDNA encoding RFP-lamin A [*Lmna*$^{-/-}$ (+ lma)]. Error bars indicate s.e.m., $n \geq 14$.

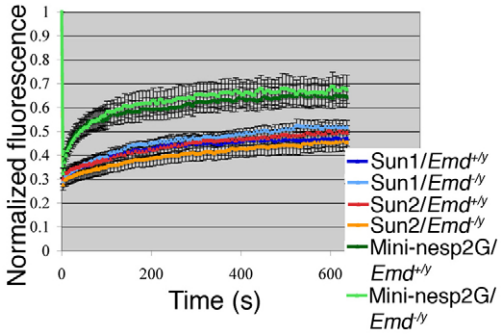

Fig. 4. Mobility of LINC complex proteins is not altered in MEFs lacking emerin. Quantitative experiments, as described in Fig. 2, showing normalized fluorescence recovery after photobleaching in wild-type MEFs (*Emd*$^{+/y}$) or *Emd*$^{-/y}$ MEFs (*Emd*$^{-/y}$) of Sun1, Sun2 and mini-nesprin-2G (Mini-nesp2G) expressed as GFP-fusion proteins. Error bars indicate s.e.m., $n \geq 12$.

recovery dynamics similar to those in wild-type MEFs, indicating that lamin A contributed to the immobilization of Sun1 in the nuclear envelope (Fig. 3A). Co-expression of RFP-lamin C, however, did not rescue the wild-type phenotype (data not shown). GFP-Sun2 and GFP-mini-nesprin-2G were also more mobile in MEFs lacking the A-type lamins. However, in these cases, co-expression with RFP-lamin A (Fig. 3B,C) or RFP-lamin C (data not shown) did not rescue the recovery dynamics. Similarly, Crisp and colleagues reported an inability of lamin A and/or C to rescue loss of Sun2 from the nuclear envelope in *Lmna*$^{-/-}$ MEFs (Crisp et al., 2006).

We performed FRAP in MEFs from emerin null mice (Melcon et al., 2006). There were no significant differences between the localization (data not shown) or mobility (Fig. 4) of GFP-Sun1, GFP-Sun2 or GFP-mini-nesprin-2G in MEFs lacking emerin and wild-type MEFs. These results indicate a role for A-type lamins, but not for emerin, in the immobilization of the LINC complex at the nuclear envelope.

Lamin A is more closely associated with Sun1 than with Sun2

To compare the molecular interactions of lamin A with Sun1 and Sun2 in intact cells, we used fluorescence resonance energy transfer (FRET) acceptor photobleaching. In this method, the increase in donor fluorescence after acceptor photobleaching is a measure of the FRET efficiency. Wild-type MEFs were co-transfected with constructs encoding RFP–lamin-A and GFP-Sun1 or GFP-Sun2. The fluorescent tags are situated in the nucleoplasm because both lamin A and Suns are tagged at their N-termini. The energy transfer between GFP-Sun1 and RFP–lamin-A was higher than the transfer between GFP-Sun2 and RFP–lamin-A (Fig. 5A,B). This indicates a closer association of lamin A with Sun1 than with Sun2. Control experiments were performed to exclude binding of lamin A or Suns to the fluorescent tags (Fig. 5B). As shown in Fig. 5C, there is no positive correlation between energy transfer and acceptor density (RFP fluorescence). Because a positive correlation is characteristic for random proximity effects, this suggests that the binding between lamin A and Suns is specific (Kenworthy, 2001; Periasamy et al., 2008).

Sun2 is necessary for the immobilization of nesprin at the nuclear envelope

To test the hypothesis that Sun1 and/or Sun2 act as connectors between lamins and nesprins, we examined the effect of the Suns on the mobility of GFP-mini-nesprin-2G. As Sun1 or Sun2 knockout MEFs were not available to us, we used RNAi to knock down Sun1 and Sun2 in wild-type MEFs co-transfected with cDNA encoding GFP-mini-nesprin-2G. We also used RNAi against emerin. To make sure that the cells examined using FRAP had taken up the siRNAs, we co-transfected cells with Block-iT Alexa Red Fluorescent Oligos. Control experiments showed a high correlation between red fluorescent oligonucleotide uptake and RNAi knockdown in co-transfected cells (Fig. 6A, lower row), whereas cells transfected with red fluorescent oligonucleotides alone showed normal levels of endogenous Suns and emerin (Fig. 6A, upper row). We therefore exclusively examined cells transfected with the red fluorescent oligonucleotide in our FRAP experiments. Two different siRNAs against Sun1 and Sun2 were used. The mobility of mini-nesprin-2G

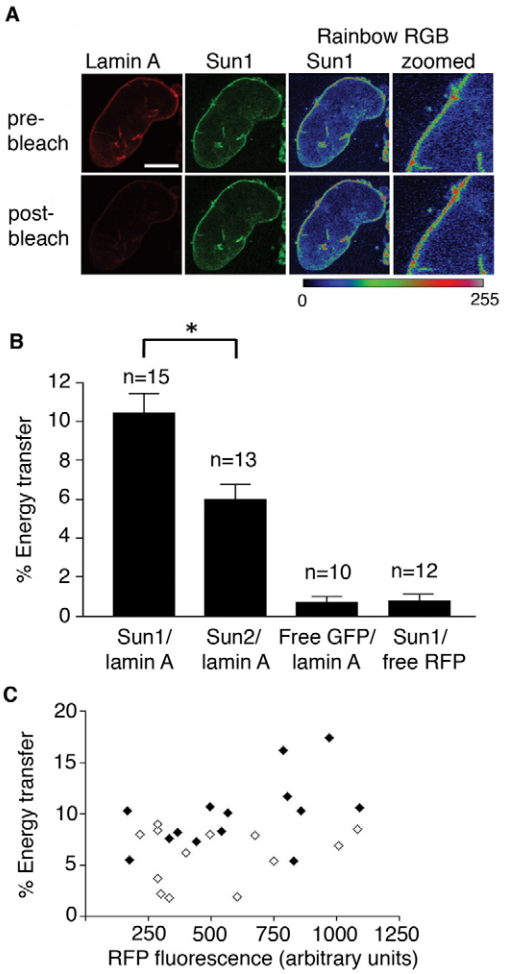

Fig. 5. Energy transfer between GFP-Sun1 and RFP–lamin-A is higher than that between GFP-Sun2 and RFP–lamin-A. Acceptor photobleaching FRET was measured in MEFs coexpressing either GFP-Sun1 or GFP-Sun2 and RFP–lamin-A. (A) Representative images of one cell expressing GFP-Sun1 and RFP–lamin-A before and after RFP photobleaching. The magnified images (far right panels) clearly demonstrate an increase in GFP fluorescence after RFP photobleaching. Scale bar: 5 µm. (B) Calculated FRET efficiencies between Sun1/lamin A and Sun2/lamin A. Error bars denote s.e.m. Unpaired, two-tailed Student's *t*-test was used for statistical significance, **P*=0.0017. Free GFP/lamin A and Sun1/free RFP were used as negative controls. (C) RFP–lamin-A (acceptor) fluorescence intensities prior to photobleaching were plotted against their corresponding FRET efficiencies for Sun1 and Sun2 to ensure that the binding between Suns and lamin A is specific. Black diamonds denote energy transfer for Sun1/lamin A and white diamonds denote energy transfer for Sun2/lamin A.

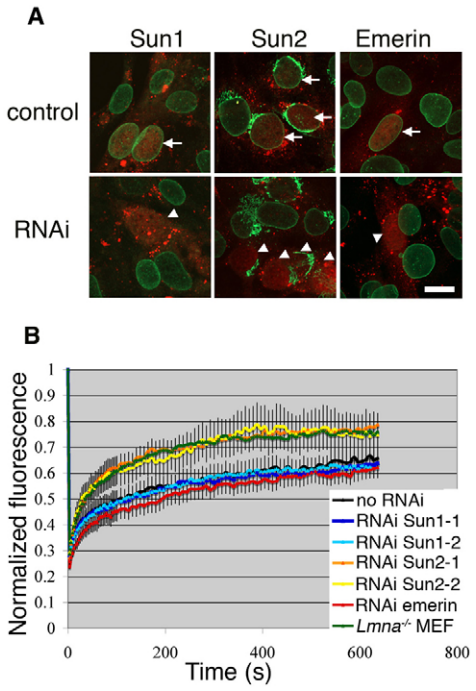

Fig. 6. RNAi knockdown of Sun2, but not of Sun1 or emerin, increases the mobility of GFP-mini-nesprin-2G in the nuclear envelope. (A) Lower panels: wild-type MEFs were co-transfected with Block-iT Alexa Red Fluorescent Oligos and siRNA oligonucleotides against Sun1 (left), Sun2 (middle) or emerin (right). Upper panels show wild-type MEFs transfected with Alexa Red Fluorescent Oligos alone, without addition of siRNAs. Laser scanning confocal immunofluorescence microscopy was performed using rabbit polyclonal antibodies against Sun1 (left panels) or Sun2 (middle panels), or mouse monoclonal antibodies against emerin (right panels). Primary antibodies were recognized by FITC-conjugated secondary antibodies. The images show an overlay of the FITC (green) and Alexa (red) channels. There is a high correlation between red fluorescent oligonucleotide uptake (arrowheads, lower panels) and knockdown of endogenous Sun1, Sun2 or emerin. Uptake of Block-iT Alexa Red Fluorescent Oligos alone (arrows, upper panels) does not affect levels of endogenous Sun1, Sun2 or emerin. Scale bar: 10 µm. (B) Quantitative experiments, as described in Fig. 2, showing normalized fluorescence recovery after photobleaching of GFP-mini-nesprin-2G in wild-type MEFs co-transfected with cDNA encoding GFP-mini-nesprin-2G, Block-iT Alexa Red Fluorescent Oligos and siRNA against Sun1, Sun2 or emerin. For Sun1 and Sun2, two different sets of siRNA oligonucleotides each were used (Sun1-1 and 1-2, and Sun2-1 and 2-2, respectively). Only cells showing uptake of Block-iT Alexa Red Fluorescent Oligos were bleached. For comparison, results from wild-type MEFs (no RNAi) and MEFs lacking A-type lamins (*Lmna*$^{-/-}$ MEF) not subjected to RNAi are also shown. Error bars indicate s.e.m., $n \geq 10$.

in MEFs depleted of Sun2 was similar to the dynamics measured in MEFs lacking A-type lamins. No difference was seen between control cells and cells subjected to RNAi against Sun1 or emerin (Fig. 6B).

Interactions between Suns and the nesprin-2 KASH domain

To determine whether the nesprin-2 KASH domain displayed preferential binding for either Sun1 or Sun2, we examined the respective direct interactions using surface plasmon resonance (Biacore). We coupled a synthetic KASH peptide to a sensor chip using amide coupling and injected glutathione-*S*-transferase (GST)-fusion proteins of the luminal domain of either Sun1 or Sun2 at various concentrations (Fig. 7A,B). Fitting of the steady-state response versus concentration of Sun protein as a standard bimolecular interaction revealed that Sun1 and Sun2 bound the nesprin-2 KASH domain with similar affinities of 0.38±0.04 µM and 0.45±0.05 µM, respectively (Fig. 7C). There was no interaction between the KASH peptide and GST alone (data not shown). We also fit the dissociation phase of the data as a single-phase decay and found that Sun1 and Sun2 dissociated from KASH with similar half-lives of 2±1 and 5±2 seconds, respectively (Fig. 7D).

The luminal region of mini-nesprin-2G is essential for outer nuclear membrane localization and immobilization, whereas the actin-binding CH region is not essential

Nesprin-2 giant has an N-terminal region that interacts with actin (Zhen et al., 2002). To investigate whether this interaction influenced

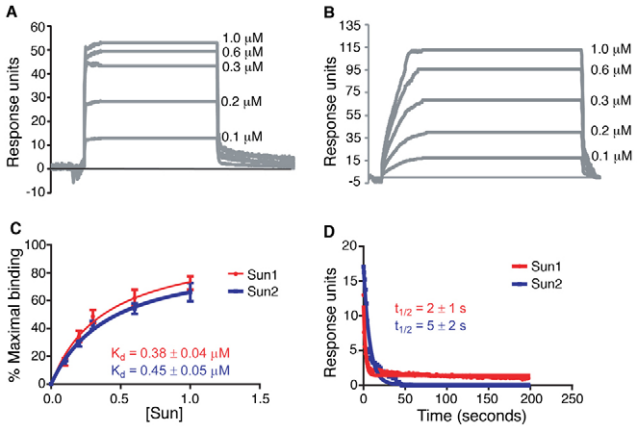

Fig. 7. The affinities between the nesprin-2 KASH domain and the luminal domains of Sun1 or Sun2 are very similar. Sensograms from Biacore experiments examining the interaction between (A) Sun1 and the nesprin-2 KASH domain and (B) the interaction between Sun2 and the nesprin-2 KASH domain. (C) Equilibrium binding analysis. Percent maximal binding at steady state (steady-state response units at a given concentration as a percentage of the maximum achievable steady-state response units) was plotted against the concentration of SUN-domain protein that was injected and the data was fit as a simple bimolecular interaction to determine the apparent binding affinity (K_d). (D) Dissociation kinetics of both Sun1 (red) and Sun2 (blue) from the nesprin-2 KASH domain. Response units were plotted against time and the data fit as a single-phase dissociation. Note that in this figure $t_{1/2}$ is the dissociation half-life (time to 50% dissociation).

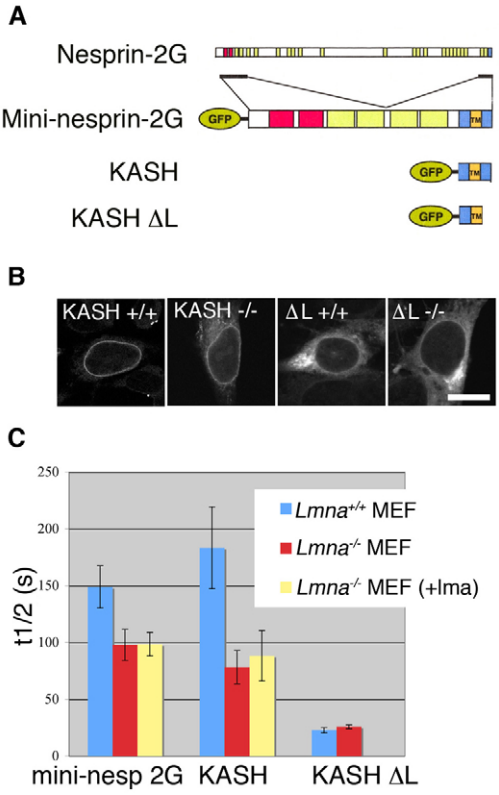

Fig. 8. The KASH domain is necessary and sufficient to immobilize mini-nesprin-2G in the nuclear envelope of MEFs. (A) Schematic depiction of GFP-mini-nesprin-2G, the GFP-tagged KASH domain of nesprin-2, and the GFP-tagged KASH domain lacking the luminal region (KASH ΔL). Diagram of full-length nesprin-2G is shown on top to indicate portions of the protein in each GFP-fusion construct. Red boxes denote CH domain; yellow boxes, spectrin repeats; and blue and orange boxes, the KASH domain with orange showing the transmembrane-spanning segment. (B) Localization of GFP-KASH and GFP-KASH ΔL in transiently transfected wild-type (+/+) or *Lmna* knockout (–/–) MEFs. Panels show laser scanning confocal microscopy images of representative transiently transfected MEFs. Scale bar: 10 μm. (C) Recovery rates are expressed in terms of $t_{1/2}$ (see Materials and Methods) for FRAP of GFP-mini-nesprin-2G, GFP-KASH or GFP-KASH ΔL in the nuclear envelope region of wild-type MEFs (blue columns), $Lmna^{-/-}$ MEFs (red columns) or $Lmna^{-/-}$ cells co-transfected with exogenous RFP-lamin A (yellow columns). Error bars indicate s.e.m., $n \geq 9$. The Student's *t*-test showed significant differences between $t_{1/2}$ in wild-type MEFs and $Lmna^{-/-}$ MEFs for GFP-mini-nesprin-2G (P=0.029) and GFP-KASH (P=0.019), but not for GFP-KASH ΔL (P=0.33). There were no significant differences in $t_{1/2}$ between $Lmna^{-/-}$ MEFs expressing or not expressing exogenous RFP-lamin A for either GFP-mini-nesprin-2G (P=0.97) or GFP-KASH (P=0.73). The $t_{1/2}$ for GFP-KASH and for GFP-KASH ΔL were significantly different in both wild-type (P =0.0097) and $Lmna^{-/-}$ (P=0.019) MEFs.

the mobility of GFP-mini-nesprin-2G, which has been shown to interact with actin (Luxton, G. W., E.R.G., E.S.F., Vintinner, E. and G.G.G., unpublished results), we transfected $Lmna^{+/+}$ and $Lmna^{-/-}$ MEFs with cDNAs encoding GFP fused to the KASH domain of nesprin-2 (Fig. 8A). We also transfected cells with GFP fused to the KASH domain lacking the luminal domain (KASH ΔL; Fig. 8A). KASH ΔL localization to the nuclear envelope in $Lmna^{+/+}$ MEFs and in $Lmna^{-/-}$ MEFs was similar to that seen for mini-nesprin-2G (Fig. 8B). By contrast, KASH ΔL did not localize to the nuclear envelope but was found throughout the endoplasmic reticulum in both $Lmna^{+/+}$ and $Lmna^{-/-}$ cells (Fig. 8B). When FRAP was performed, there were no significant differences between the $t_{1/2}$ of KASH and mini-nesprin-2G, either in $Lmna^{+/+}$ cells or in $Lmna^{-/-}$ cells with or without expression of RFP-lamin A (Fig. 8C). As shown above for GFP-mini-nesprin-2G, the KASH domain had a significantly faster recovery in $Lmna^{-/-}$ MEFs than in $Lmna^{+/+}$ cells, and exogenous RFP-lamin A could not rescue the wild-type phenotype. Similar results were obtained in cells transfected with cDNAs encoding GFP-mini-nesprin-2G with the actin-binding CH domain deleted, as well as GFP-mini-nesprin-2G with point mutations that abolish actin-binding in the CH domain (data not shown). KASH ΔL had a low $t_{1/2}$ (quick recovery), with no significant difference in $Lmna^{+/+}$ or $Lmna^{-/-}$ cells (Fig. 8C). These experiments indicate that the luminal region of mini-nesprin-2G is necessary for its localization and immobilization at the nuclear envelope and that binding to actin has no gross effect on the diffusional mobility of the protein in this cellular compartment.

Discussion

Movement of the nucleus within the cytoplasm is crucial for cellular events such as migration, differentiation, polarization, meiosis and mitosis. Such movement requires interactions between the nucleus and cytoskeletal systems (Wilhelmsen et al., 2006). Nesprin-1 is necessary for anchoring of nuclei at specific sites in mammalian muscle cells (Grady et al., 2005; Zhang et al., 2007b) and actin is important for nuclear positioning in migrating mammalian fibroblasts (Gomes et al., 2005). Disruption of the LINC complex leads to a loss of mechanical stiffness in Swiss3T3 cells, similar to that seen in $Lmna^{-/-}$ fibroblasts (Broers et al., 2004; Lammerding et al., 2004; Lee et al., 2007; Stewart-Hutchinson et al., 2008). $Lmna^{-/-}$ fibroblasts also have defects in migration and polarization (Houben et al., 2009; Lee et al., 2007). These findings all point to a role for the LINC complex as a linker between the nucleoskeleton

and cytoskeleton and that it has a function in nuclear positioning within cells.

Studies in mammalian cells have indicated a role for lamins and Suns in the localization of nesprins to the nuclear envelope (Houben et al., 2009; Libotte et al., 2005; Muchir et al., 2003; Padmakumar et al., 2005; Zhang et al., 2005). However, most studies have failed to show a role for A-type lamins in the localization or retention of Suns (Crisp et al., 2006; Haque et al., 2006; Hasan et al., 2006). This is intriguing because Suns are likely to facilitate the indirect interaction between the lamina and nesprins (Crisp et al., 2006). To detect subtle changes in protein localization and retention, we preformed FRAP. We found that both Sun1 and Sun2 are relatively immobile in the inner nuclear membrane, with dynamics similar to LBR, which has been shown to interact with both B-type lamins and chromatin (Ye and Worman, 1994; Ye et al., 1997). To study nesprin-2 giant, the large size of which makes cloning a full-length cDNA difficult, we used mini-nesprin-2G, which is a short, artificial form containing the actin-binding CH domain, the KASH domain and spectrin repeats flanking the KASH domain. Mini-nesprin-2G was more mobile than the Suns, but not as mobile as emerin in the nuclear envelope. One limitation of our results is that the mobility of full-length nesprin-2 giant might also be affected by protein-protein interactions within spectrin repeats not present in mini-nesprin-2G (Simpson and Roberts, 2008). Future studies using nesprin-2 constructs of different length are needed to address the role of different spectrin repeats in the mobility of nesprin-2 and in its localization to the nuclear envelope.

Our results show that although both Suns and mini-nesprin-2G localize to the nuclear envelope in cells lacking A-type lamins, the proteins are less tightly retained there than in wild-type cells. These findings differ from those of Hasan and colleagues, who reported that the lateral mobility of Sun1 was unaffected in HeLa cells treated with RNAi against A-type and B-type lamins (Hasan et al., 2006). These different observations could be due to differences between cell types or, more probably, occur because the small amounts of lamins remaining after RNAi treatment are sufficient for the immobilization of Sun1 at the nuclear envelope. To compare the association of Sun1 and Sun2 with lamin A in vivo, we performed FRET. Our data obtained using FRET suggest a higher affinity between Sun1 and lamin A than between Sun2 and lamin A. This could explain why RFP-lamin A expression in cells lacking endogenous lamin A decreased the mobility of Sun1, but not of Sun2.

Because emerin has been reported to interact with at least some nesprin isoforms (Libotte et al., 2005; Mislow et al., 2002a; Zhang et al., 2005), we studied mini-nesprin-2G and Sun mobility in MEFs lacking emerin, and in wild-type MEFs treated with RNAi against emerin. There were no discernable differences between Sun or mini-nesprin-2G motility in these cells. Although we cannot rule out the possibility that emerin interacts with regions of nesprin-2 giant not present in the shorter construct that we used (Wheeler et al., 2007), our results suggest that emerin is not necessary for anchoring of LINC complex protein. Mini-nesprin-2G was also correctly localized to the nuclear envelope, as reported for nesprin-2 in dermal fibroblasts lacking emerin (Libotte et al., 2005). In our studies, RNAi knockdown of Sun2 was sufficient to increase the mobility of mini-nesprin-2G in the nuclear envelope, whereas knockdown of Sun1 had no apparent effect. It is possible that the difference in mini-nesprin-2G mobility between cells with Sun1 or Sun2 knockdown is due to differences in RNAi efficiency. Another possibility is that Sun2, but not Sun1, anchors GFP-mini-nesprin-2G. This is in agreement with our finding that plasmid-mediated expression of lamin A could immobilize GFP-Sun1, but not GFP-Sun2 or GFP-mini-nesprin-2G, in *Lmna*$^{-/-}$ MEFs. Our results support the hypothesis that Suns, at least Sun2, tether nesprin-2 to the nuclear envelope, forming a connection between lamins and nesprins. One previous study showed Sun1 to be required for proper nuclear envelope localization of nesprin-2 in HaCaT keratinocytes (Padmakumar et al., 2005). Another study showed little effect on localization of outer nuclear membrane nesprin-2 giant in HeLa cells when Sun1 or Sun2 were depleted with RNAi, but showed an 80% reduction of nesprin-2 giant from the nuclear envelope when they were co-depleted (Crisp et al., 2006). These findings might reflect varying efficiency of the RNAi, or different roles for the various Suns in different cell types. At this time, no comprehensive study has quantified the levels of all LINC complex components in different cell types and tissues.

In mammalian cells, Sun1 and Sun2 have been shown to interact with the KASH domain of nesprins in immunoprecipitation experiments. Both the SUN domain and regions upstream of it have been implicated in this interaction (Crisp et al., 2006; Padmakumar et al., 2005). Previous studies have shown that the KASH domain is necessary and sufficient for localization of nesprins to the nuclear envelope (Libotte et al., 2005; Padmakumar et al., 2005; Wilhemsen et al., 2005; Zhang et al., 2001; Zhen et al., 2002). We have shown that this region is also sufficient for reducing the diffusional mobility of mini-nesprin-2G in the nuclear envelope. The actin-binding CH domain has no effect on the bulk diffusional mobility of mini-nesprin-2G.

The KASH domains from nesprins 1, 2 and 3 interact promiscuously with the luminal domains of Sun1 and Sun2 (Stewart-Hutchinson et al., 2008). However, it is not clear to what extent the Suns are interchangeable. For instance, Sun1 but not Sun2, is required for the proper retention of nesprin-3α at the outer nuclear membrane (Ketema et al., 2007). We measured the affinities of Sun1 and Sun2 with the luminal region of nesprin-2 in vitro using plasmon surface resonance. FRET was not feasible because the relatively large fluorescent tags would probably interfere with the Sun-KASH interaction, which requires a free C-terminal end on the KASH domain (Stewart-Hutchinson et al., 2008). Sun1 and Sun2 bound to the nesprin-2 KASH domain with nearly identical affinities of 0.38±0.04 μM and 0.45±0.05 μM, respectively, suggesting that the differences between the ability of these proteins to anchor mini-nesprin-2G observed in our RNAi experiments are not due to differences in direct protein-protein interactions. We therefore examined whether there is a difference in the stability of the KASH-Sun1 and KASH-Sun2 complexes. Sun1 dissociated from KASH with a half-life of 2±1 seconds, whereas Sun2 dissociated from KASH with a half-life of 5±2 seconds. Although these half-lives of dissociation are different, both represent rapid dissociation, further suggesting that the differences found by FRAP experiments are not due to the differences in the intrinsic interactions between Sun1 or Sun2 and the KASH domain. Other proteins, as well as dimerization or multimerization of the LINC complex proteins, might strengthen or modulate the interactions in vivo and thereby enable the LINC complex to transmit force across the nuclear membrane.

The affinities we measured for binding between the luminal domains of the Suns and the nesprin-2 KASH domain are higher than those previously determined between F-actin and the actin-binding domain of nesprin-1 giant and nesprin-2 giant. These have been measured as 5.7±1.2 μM and 3.8±1 μM, respectively, using high-speed co-sedimentation assays (Padmakumar et al., 2004; Zhen

et al., 2002). A more robust interaction of nesprins to the nucleus than to actin could be expected if nesprins function as an attachment site on the nucleus, enabling the dynamic actin network to move the nucleus and indirectly interact with the nucleoskeleton (Luxton, G. W., E.R.G., E.S.F., Vintinner, E. and G.G.G., unpublished results).

Mutations in the *LMNA* gene encoding A-type lamins cause a wide spectrum of diseases, sometimes called laminopathies (Worman and Bonne, 2007). Many of the laminopathies (e.g. Emery-Dreifuss muscular dystrophy) affect striated muscle, but lipodystrophies, premature aging syndromes and other disorders are also caused by *LMNA* mutations. As LINC complex proteins are components of the nuclear envelope that interact with lamins, they might play a role in the pathogenesis of these diseases as a result of altered interactions with variant lamins. Mutations in genes encoding LINC complex proteins could also directly result in disease (Gros-Louis et al., 2007; Zhang et al., 2007a).

Two non-exclusive hypotheses have been proposed to explain how mutations in genes encoding lamins and other nuclear envelope proteins cause disease. One hypothesis is that mutations cause structural changes in the nuclei and cytoskeleton, rendering cells more susceptible to mechanical stress; the other is that the mutations somehow lead directly to abnormal gene expression (Capell and Collins, 2006; Worman and Courvalin, 2004; Worman and Bonne, 2007). Cells in which LINC complexes are disrupted show a loss of cellular stiffness similar to that measured in cells lacking A-type lamins (Lammerding et al., 2004; Lee et al., 2007; Stewart-Hutchinson et al., 2008). This suggests that the LINC complex might play a role in preventing susceptibility to damage by mechanical stress. Mis-sense mutations or polymorphisms in *SYNE1* and *SYNE2* (which encode nesprins 1 and 2) have been identified in probands with Emery-Dreifuss muscular dystrophy-like phenotypes, and fibroblasts from these subjects show defects in localization of nesprin, lamin, emerin and Sun2 (but not Sun1) (Zhang et al., 2007a). Mice with the KASH domain of nesprin-1 deleted also exhibit an Emery-Dreifuss muscular dystrophy-like phenotype and perinatal death (Puckelwartz et al., 2009). Further studies on the functions of LINC complex components and their interactions with other proteins could therefore provide insights into the mechanisms underlying disease.

Materials and Methods

Plasmid construction

cDNA encoding full-length murine Sun1 (GenBank accession number BC047928) was digested with *Sal*I and *Bam*HI and ligated into the *Sal*I/*Bam*HI sites of vector EGFP-C1 (Clontech Laboratories, Mountain View, CA). Murine Sun2 (GenBank accession number AY682987) cDNA was amplified from NIH 3T3 cells using Thermoscript RT-PCR System (Invitrogen) with 5′-primer 5′-TACGCGTCGACA-TGTCGAGACGAAGCCAGC-3′ and 3′-primer 5′-CGTCTAGAAGACTAGTG-GGCAGGCTCTC-3′. The cDNA was digested with *Sal*I and *Xba*I and ligated into the *Sal*I/*Xba*I sites of EGFP-C1. Mini-nesprin-2G was constructed by the insertion of murine nesprin-2 (RefSeq NM_001005510) cDNA, encoding amino acids 3-485 and 6525-6874, into the *Sal*I/*Xba*I sites of EGFP-C1. To fuse the N-terminal and C-terminal fragments we performed an overlapping PCR (Sambrook and Russell, 2001) using the following: 5′-primer 5′-GCTAGCCCTGTGCTGCCCA-3′, 5′ overlap primer 5′-CTTCATCCCACTCCTGGAGCTTCACAGCAAGC-3′, 3′ overlap primer 5′-GCTTGCTGTGAAGCTCCAGGAGTGGGATGAAG-3′, and 3′-primer 5′-CTA-GGTGGGAGGTGGCCCGTT-3′. Truncated nesprin cDNAs were amplified by PCR using mini-nesprin-2G as a template and ligated into *Xho*I/*Eco*RI sites of EGFP-C1. GFP-mini-nesprin-2G variants with point mutations (I128A and I131A) were generated using Quickchange site-directed mutagenesis kit (Stratagene, La Jolla, CA) with 5′-primer 5′-CCATTATCCTTGGCCTGGCTTGGACCGCTATCCTGCAC-TTTCATATTG-3′ and 3′-primer 5′-CAATATGAAAGTGCAGGATAGCGGTCC-AAGCCAGGCCAAGGATAATGG-3′. cDNA encoding RFP-lamin A, emerin-GFP and LBR-GFP have been described previously (Ellenberg et al., 1997; Östlund et al., 1999; Östlund et al., 2006). RFP-Lamin C was generated by ligating lamin C cDNA from plasmid pS65T-C1 (Broers et al., 2005) digested with *Bam*HI and *Xho*I into RFP-C1 digested with the same enzymes. For Biacore experiments, cDNA encoding the luminal domains of Sun1 (amino acids 432-913) and Sun2 (amino acids 239-729) were amplified by PCR using the appropriate primers and Sun1 or Sun2 cDNAs in EGFP-C1 as templates. The PCR products were then ligated into the *Bam*HI/*Eco*RI sites (Sun1) or *Eco*RI/*Xho*I sites (Sun2) of vector pGEX-4T (GE Healthcare, Piscataway, NJ), with the resulting plasmids encoding GST-Sun fusion proteins. All cloning procedures were performed according to standard methods and all constructs were verified by DNA sequencing at the Protein Core Facility, Columbia University, NY.

Cell culture, transfection and RNAi

Immortalized MEFs from wild-type, $Lmna^{-/-}$ and $Emd^{-/y}$ mice, provided by Colin Stewart, Institute of Medical Biology, Singapore (Melcon et al., 2006; Sullivan et al., 1999) were grown in Dulbecco's modified Eagle's medium (DMEM) containing 10% fetal bovine serum at 37°C and 5% CO_2. For FRAP, cells were transfected in chambered coverglasses (Nalge Nunc International, Rochester, NY) using Lipofectamine PLUS (Invitrogen, Carlsbad, CA), following the manufacturer's instructions. Cells were overlaid with the lipid-DNA complexes for 23 hours, the 4 first of which were in serum-free media (Invitrogen). Cells were grown for an additional 16-40 hours before the photobleaching experiments. For knockdown of Sun1 and Sun2, we used Stealth Select RNAi duplexes (Invitrogen) and for knockdown of emerin, FlexiTube siRNA (Qiagen, Valencia, CA). For FRAP, wild-type fibroblasts were grown in DMEM with 10% fetal bovine serum in eight-well coverglasses overnight. The cells were then transfected with the Stealth Select RNAi together with BLOCK-it Alexa Fluor Red Fluorescent Oligo (Invitrogen) and GFP-mini-nesprin-2G cDNA, using Lipofectamine PLUS (Invitrogen) in serum-free media, according to the manufacturer's instructions. After 4 hours, serum was added to a concentration of 10% and the cells were then grown for an additional 44-68 hours before the photobleaching experiments. For control of RNAi knockdown efficiency, cells grown as above in eight-well chamberslides were transfected with the Stealth Select RNAi together with BLOCK-it Alexa Fluor Red Fluorescent Oligo. After 48 hours, immunofluorescence was performed as described below.

Immunofluorescence microscopy

For Triton X-100 permeabilization, cells were washed three times with phosphate-buffered saline (PBS) and then fixed with methanol for 6 minutes at –20°C. Cells were permeabilized with 0.5% Triton X-100 in PBS for 2 minutes at room temperature, washed three times with 0.1% Tween-20 in PBS and incubated with the primary antibodies diluted in PBS containing 0.1% Tween-20 and 2% bovine serum albumin for 1 hour at room temperature. After four washes with 0.1% Tween-20 in PBS, the cells were incubated with the secondary antibodies diluted 1:200 as described for the primary antibodies. The cells were then washed twice with PBS containing 0.1% Tween-20 and twice with PBS. The slides were dipped in methanol, air-dried and mounted using SlowFade Light Anti-fade Kit (Invitrogen). For digitonin permeabilization, the transfected cells were washed three times with PBS and fixed with 2% paraformaldehyde in PBS for 30 minutes on ice. They were washed three times with PBS and then incubated with precooled 40 μg/ml digitonin (Calbiochem, La Jolla, CA) in PBS for 10 minutes on ice. The cells were then washed and incubated with antibodies as described above, except that Tween-20 was excluded from the buffers and all steps were performed on ice.

Primary antibodies used were mouse monoclonal anti-emerin antibody (Vector Laboratories, Burlingame, CA) at a dilution of 1:30; rabbit anti-Sun1 antibody, a gift from Min Han, University of Colorado, Boulder, CO (Ding et al., 2007) at a dilution of 1:500; rabbit anti-Sun2 antibody, a gift from Didier Hodzic, Washington University School of Medicine, St Louis, MO (Hodzic et al., 2004) at a dilution of 1:1000; and rabbit anti-GFP antibody (ab290; Abcam, Cambridge, MA) at a dilution of 1:1000. Secondary antibodies used were lissamine rhodamine-B-conjugated goat anti-rabbit IgG, fluorescein isothiocyanate (FITC)-conjugated goat anti-mouse IgG and FITC-conjugated goat anti-rabbit IgG. Immunofluorescence microscopy, FRAP and FRET were performed on a Zeiss Axiovert 200 M microscope attached to a Zeiss LSM 510 confocal laser scanning system (Carl Zeiss, Thornwood, NY).

Fluorescence recovery after photobleaching

FRAP was performed using the 488 nm line of a 30 mW argon laser in conjunction with a 40× 1.3 numerical aperture objective. The bleached area was photobleached at full laser power (100% transmission) for 25 iterations and recovery of photobleaching monitored by scanning at low power (5% transmission) in 2-second intervals. The average intensity of the fluorescence signal was measured in the region of interest using NIH ImageJ software (http://rsb.info.nih.gov/ij/). It was then normalized to the change in total fluorescence as $I_{rel}=T_0I_t/T_tI_0$ where T_0 is total cellular intensity during prebleach, T_t total cellular intensity at time point t, I_0 the average intensity in the bleach-region during prebleach and I_t the average intensity in the bleach-region at time point t (Phair and Misteli, 2000). The normalized fluorescence was then plotted against time after bleaching.

As the immobile fraction (the difference between the fluorescence intensity in the bleached area prebleach and the intensity at infinity after bleach) was different for the different proteins and cell types, we used a modified time of half-recovery value

($t_{1/2}$), where $t_{1/2}$ is the time after bleach required for the fluorescence levels to reach the median between levels immediately after bleach and prebleach, rather than using the median between prebleach levels and steady-state levels. To determine $t_{1/2}$, we used a modification of the method described by Harrington and colleagues (Harrington et al., 2002). We plotted $\ln(1-i_t)$ versus time after bleach, where i_t is the average normalized fluorescence intensity in the bleach-region at time t and 1 is the average normalized fluorescence intensity in the bleach-region prebleach. The curves were fitted using KaleidaGraph (http://www.synergy.com) and $t_{1/2}$ calculated as $t_{1/2}=\ln 2\times(-1/\text{slope})$. Data from the first 31 seconds after bleach were used in all experiments.

Fluorescence resonance energy transfer

FRET acceptor photobleaching was performed as described by Kenworthy (Kenworthy, 2001). Immortalized MEFs grown in chamberslides were co-transfected with expression vectors encoding either EGFP-fused Sun1 or Sun2 (donor) and RFP-lamin A (acceptor). The cells were fixed in ice-cold methanol for 5 minutes and rehydrated with PBS. The RFP signal was destroyed by repeatedly photobleaching of the whole cell using the 543 nm line of a helium-neon laser at 100% laser output. Cells displaying comparable levels of GFP and RFP fluorescence were selected for FRET analysis in which images in both channels were obtained before and after acceptor photobleaching. The nuclear lamina was selected as the region of interest and the energy transfer efficiency E was calculated on a pixel-by-pixel basis using the equation $100\times(1-\text{GFP}_{\text{PRE}}/\text{GFP}_{\text{POST}})$, where GFP_{PRE} denotes GFP fluorescence before acceptor photobleaching and GFP_{POST} denotes that after acceptor photobleaching. The data analysis and the calculation of E were performed using the ImageJ software (Abramoff et al., 2004) with the AccPbFRET plugin (Roszik et al., 2008).

Biacore experiments

Plasmon surface resonance experiments were performed using Biacore X (Biacore AB, Uppsala, Sweden). A peptide containing the luminal region of the nesprin-2 KASH domain (SEDDYSCTQANNFARSFYPMLRYTNGPPPT; Peptide 2.0, Chantilly, VA) was dissolved in HBS-P buffer (Biacore AB) with the pH adjusted by the addition of Tris-HCl pH 9. KASH peptide (1.1 mM) was diluted 1:2 with acetate buffer pH 5.5 (Biacore AB) and then coupled to a CM5 sensor chip (Biacore AB) by standard amide coupling protocols using the Amine Coupling Kit (Biacore AB). Coupling was between 500 and 700 response units. Active sites on the sensor chip were blocked with ethanolamine (Biacore AB) prior to injection of GST-Sun1 or GST-Sun2. GST-Sun fusion proteins were expressed in *Escherichia coli* strain BL21 and purified on a glutathione Sepharose column according to the manufacturer's instructions (GE Healthcare). Suns in HBS-P buffer pH 7.5 were injected at concentrations ranging from 0.1 μM to 1 μM at a flow rate of 10 μl/minute. Background signal from an empty flow cell was subtracted and the steady-state response for each concentration of Sun1 and Sun2 was determined using BiaEvaluation (Biacore AB). Percent maximal binding at the plateau was then plotted against the concentration of Sun protein injected and the affinities determined by fitting the data as a standard bimolecular interaction ($Y=B_{\max}*X/K_d+X$) using Prism 5 software (GraphPad Software, La Jolla, CA). Details of the analysis are described elsewhere (Folker et al., 2005). For kinetic analysis the dissociation following the completion of the injection was fit as a single-phase dissociation ($Y=Y_{\max}*e^{-kx}$) using Prism 5 software. Dissociation experiments performed at a flow rate of 25 μl/minute resulted in the same dissociation rate constant, indicating that rebinding was not causing an artificially slow dissociation.

Supported by NIH grant NS059352. We thank Didier Hodzic and Min Han for antibodies, Colin Stewart for mouse embryonic fibroblasts and Renjun Pei for help with the Biacore experiments. Deposited in PMC for release after 12 months.

References

Abramoff, M. D., Magelhaes, P. J. and Ram, S. J. (2004). Image processing with ImageJ. *Biophotonics Int.* **11**, 26-42.

Adam, S. A., Sterne-Marr, R. and Gerace, L. (1992). Nuclear protein import using digitonin-permeabilized cells. *Methods Enzymol.* **219**, 97-110.

Apel, E. D., Lewis, R. M., Grady, R. M. and Sanes, J. R. (2000). Syne-1, a dystrophin- and Klarsicht-related protein associated with synaptic nuclei at the neuromuscular junction. *J. Biol. Chem.* **275**, 31986-31995.

Broers, J. L., Peeters, E. A., Kuijpers, H. J., Endert, J., Bouten, C. V., Oomens, C. W., Baaijens, F. P. and Ramaekers, F. C. (2004). Decreased mechanical stiffness in LMNA–/– cells is caused by defective nucleo-cytoskeletal integrity: implications for the development of laminopathies. *Hum. Mol. Genet.* **13**, 2567-2580.

Broers, J. L. V., Kuijpers, H. J. H., Östlund, C., Worman, H. J., Endert, J. and Ramaekers, F. C. S. (2005). Both lamin A and lamin C mutations cause lamina instability as well as loss of internal nuclear lamin organization. *Exp. Cell Res.* **304**, 582-592.

Capell, B. C. and Collins, F. S. (2006). Human laminopathies: nuclei gone genetically awry. *Nat. Rev. Genet.* **7**, 940-952.

Crisp, M., Liu, Q., Roux, K., Rattner, J. B., Shanahan, C., Burke, B., Stahl, P. D. and Hodzic, D. (2006). Coupling of the nucleus and cytoplasm: role of the LINC complex. *J. Cell Biol.* **172**, 41-53.

Ding, X., Xu, R., Yu, J., Xu, T., Zhuang, Y. and Han, M. (2007). SUN1 is required for telomere attachment to nuclear envelope and gametogenesis in mice. *Dev. Cell* **12**, 863-872.

Ellenberg, J., Siggia, E. D., Moreira, J. E., Smith, C. L., Presley, J. F., Worman, H. J. and Lippincott-Schwartz, J. (1997). Nuclear membrane dynamics and reassembly in living cells: targeting of an inner nuclear membrane protein in interphase and mitosis. *J. Cell Biol.* **138**, 1193-1206.

Folker, E. S., Baker, B. M. and Goodson, H. V. (2005). Interactions between CLIP-170, tubulin, and microtubules: implications for the mechanism of Clip-170 plus-end tracking behavior. *Mol. Biol. Cell.* **16**, 5373-5384.

Gomes, E. R., Jani, S. and Gundersen, G. G. (2005). Nuclear movement regulated by Cdc42, MRCK, myosin, and actin flow establishes MTOC polarization in migrating cells. *Cell* **121**, 451-463.

Grady, R. M., Starr, D. A., Ackerman, G. L., Sanes, J. R. and Han, M. (2005). Syne proteins anchor muscle nuclei at the neuromuscular junction. *Proc. Natl. Acad. Sci. USA* **102**, 4359-4364.

Gros-Louis, F., Dupre, N., Dion, P., Fox, M. A., Laurent, S., Verreault, S., Sanes, J. R., Bouchard, J. P. and Rouleau, G. A. (2007). Mutations in SYNE1 lead to a newly discovered form of autosomal recessive cerebellar ataxia. *Nat. Genet.* **39**, 80-85.

Gruenbaum, Y., Lee, K. K., Liu, J., Cohen, M. and Wilson, K. L. (2002). The expression, lamin-dependent localization and RNAi depletion phenotype for emerin in *C. elegans*. *J. Cell Sci.* **115**, 923-929.

Haque, F., Lloyd, D. J., Smallwood, D. T., Dent, C. L., Shanahan, C. M., Fry, A. M., Trembath, R. C. and Shackleton, S. (2006). SUN1 interacts with nuclear lamin A and cytoplasmic nesprins to provide a physical connection between the nuclear lamina and the cytoskeleton. *Mol. Cell. Biol.* **26**, 3738-3751.

Harrington, K. S., Javed, A., Drissi, H., McNeil, S., Lian, J. B., Stein, J. L., Van Wijnen, A. J., Wang, Y. L. and Stein, G. S. (2002). Transcription factors RUNX1/AML1 and RUNX2/Cbfa1 dynamically associate with stationary subnuclear domains. *J. Cell Sci.* **115**, 4167-4176.

Hasan, S., Guttinger, S., Muhlhausser, P., Anderegg, F., Burgler, S. and Kutay, U. (2006). Nuclear envelope localization of human UNC84A does not require nuclear lamins. *FEBS Lett.* **580**, 1263-1268.

Hodzic, D. M., Yeater, D. B., Bengtsson, L., Otto, H. and Stahl, P. D. (2004). Sun2 is a novel mammalian inner nuclear membrane protein. *J. Biol. Chem.* **279**, 25805-25812.

Houben, F., Willems, C. H., Declercq, I. L., Hochstenbach, K., Kamps, M. A., Snoeckx, L. H., Ramaekers, F. C. and Broers, J. L. (2009). Disturbed nuclear orientation and cellular migration in A-type lamin deficient cells. *Biochim. Biophys. Acta* **1793**, 312-324.

Kandert, S., Lüke, Y., Kleinhenz, T., Neumann, S., Lu, W., Jaeger, V. M., Munck, M., Wehnert, M., Muller, C. R., Zhou, Z. et al. (2007). Nesprin-2 giant safeguards nuclear envelope architecture in LMNA S143F progeria cells. *Hum. Mol. Genet.* **16**, 2944-2959.

Kenworthy, A. K. (2001). Imaging protein-protein interactions using fluorescence resonance energy transfer microscopy. *Methods* **24**, 289-296.

Ketema, M., Wilhelmsen, K., Kuikman, I., Janssen, H., Hodzic, D. and Sonnenberg, A. (2007). Requirements for the localization of nesprin-3 at the nuclear envelope and its interaction with plectin. *J. Cell Sci.* **120**, 3384-3394.

Lammerding, J., Schulze, P. C., Takahashi, T., Kozlov, S., Sullivan, T., Kamm, R. D., Stewart, C. L. and Lee, R. T. (2004). Lamin A/C deficiency causes defective nuclear mechanics and mechanotransduction. *J. Clin. Invest.* **113**, 370-378.

Lee, J. S., Hale, C. M., Panorchan, P., Khatau, S. B., George, J. P., Tseng, Y., Stewart, C. L., Hodzic, D. and Wirtz D. (2007). Nuclear lamin A/C deficiency induces defects in cell mechanics, polarization, and migration. *Biophys. J.* **93**, 2542-2552.

Lei, K., Zhang, X., Ding, X., Guo, X., Chen, M., Zhu, B., Xu, T., Zhuang, Y., Xu, R. and Han, M. (2009). SUN1 and SUN2 play critical but partially redundant roles in anchoring nuclei in skeletal muscle cells in mice. *Proc. Natl. Acad. Sci. USA* **106**, 10207-10212.

Libotte, T., Zaim, H., Abraham, S., Padmakumar, V. C., Schneider, M., Lu, W., Munck, M., Hutchison, C., Wehnert, M., Fahrenkrog, B. et al. (2005). Lamin A/C-dependent localization of Nesprin-2, a giant scaffolder at the nuclear envelope. *Mol. Biol. Cell* **16**, 3411-3424.

Liu, J., Lee, K. K., Segura-Totten, M., Neufeld, E., Wilson, K. L. and Gruenbaum, Y. (2003). MAN1 and emerin have overlapping function(s) essential for chromosome segregation and cell division in Caenorhabditis elegans. *Proc. Natl. Acad. Sci. USA* **100**, 4598-4603.

Liu, Q., Pante, N., Misteli, T., Elsagga, M., Crisp, M., Hodzic, D., Burke, B. and Roux, K. J. (2007). Functional association of Sun1 with nuclear pore complexes. *J. Cell Biol.* **178**, 785-798.

Lu, W., Gotzmann, J., Sironi, L., Jaeger, V. M., Schneider, M., Lüke, Y., Uhlen, M., Szigyarto, C. A., Brachner, A., Ellenberg, J. et al. (2008). Sun1 forms immobile macromolecular assemblies at the nuclear envelope. *Biochim. Biophys. Acta* **1783**, 2415-2426.

Lüke, Y., Zaim, H., Karakesisoglou, I., Jaeger, V. M., Sellin, L., Lu, W., Schneider, M., Neumann, S., Beijer, A., Munck, M. et al. (2008). Nesprin-2 Giant (NUANCE) maintains nuclear envelope architecture and composition in skin. *J. Cell Sci.* **121**, 1887-1898.

Melcon, G., Kozlov, S., Cutler, D. A., Sullivan, T., Hernandez, L., Zhao, P., Mitchell, S., Nader, G., Bakay, M., Rottman, J. N. et al. (2006). Loss of emerin at the nuclear envelope disrupts the Rb1/E2F and MyoD pathways during muscle regeneration. *Hum. Mol. Genet.* **15**, 637-651.

Mislow, J. M., Holaska, J. M., Kim, M. S., Lee, K. K., Segura-Totten, M., Wilson, K. L. and McNally, E. M. (2002a). Nesprin-1alpha self-associates and binds directly to emerin and lamin A in vitro. *FEBS Lett.* **525**, 135-140.

Mislow, J. M., Kim, M. S., Davis, D. B. and McNally, E. M. (2002b). Myne-1, a spectrin repeat transmembrane protein of the myocyte inner nuclear membrane, interacts with lamin A/C. *J. Cell Sci.* **115**, 61-70.

Muchir, A., van Engelen, B. G., Lammens, M., Mislow, J. M., McNally, E., Schwartz, K. and Bonne, G. (2003). Nuclear envelope alterations in fibroblasts from LMGD1B patients carrying nonsense Y259X heterozygous or homozygous mutation in lamin A/C gene. *Exp. Cell Res.* **291**, 352-362.

Östlund, C., Ellenberg, J., Hallberg, E., Lippincott-Schwartz, J. and Worman, H. J. (1999). Intracellular trafficking of emerin, the Emery-Dreifuss muscular dystrophy protein. *J. Cell Sci.* **112**, 1709-1719.

Östlund, C., Sullivan, T., Stewart, C. L. and Worman, H. J. (2006). Dependence of diffusional mobility of integral inner nuclear membrane proteins on A-type lamins. *Biochemistry* **45**, 1374-1382.

Padmakumar, V. C., Abraham, S., Braune, S., Noegel, A. A., Tunggal, B., Karakesisoglou, I. and Korenbaum, E. (2004). Enaptin, a giant actin-binding protein, is an element of the nuclear membrane and the actin cytoskeleton. *Exp. Cell Res.* **295**, 330-339.

Padmakumar, V. C., Libotte, T., Lu, W., Zaim, H., Abraham, S., Noegel, A. A., Gotzmann, J., Foisner, R. and Karakesisoglou, I. (2005). The inner nuclear membrane protein Sun1 mediates the anchorage of Nesprin-2 to the nuclear envelope. *J. Cell Sci.* **118**, 3419-3430.

Periasamy, A., Wallrabe, H., Chen, Y. and Barroso M. (2008). Quantitation of protein-protein interactions: confocal FRET microscopy. *Methods Cell Biol.* **89**, 569-598.

Phair, R. D., and Misteli, T. (2000). High mobility of proteins in the mammalian cell nucleus. *Nature* **404**, 604-609.

Puckelwartz, M. J., Kessler, E., Zhang, Y., Hodzic, D., Randles, K. N., Morris, G., Earley, J. U., Hadhazy, M., Holaska, J. M., Mewborn S. K. et al. (2009). Disruption of nesprin-1 produces an Emery Dreifuss muscular dystrophy-like phenotype in mice. *Hum. Mol. Genet.* **18**, 607-620.

Roszik, J., Szöllosi, J. and Vereb, G. (2008). AccPbFRET: an ImageJ plugin for semi-automatic, fully corrected analysis of acceptor photobleaching FRET images. *BMC Bioinformatics* **9**, 346.

Roux, K. J., Crisp, M. L., Liu, Q., Kim, D., Kozlov, S., Stewart, C. L. and Burke, B. (2009). Nesprin 4 is an outer nuclear membrane protein that can induce kinesin-mediated cell polarization. *Proc. Natl. Acad. Sci. USA* **106**, 2194-2199.

Sambrook, J. and Russell, D. W. (2001). *Molecular Cloning: A Laboratory Manual*, *Vol. 3*. Cold Spring Harbor, NY: Cold Spring Harbor Laboratory Press.

Simpson, J. G. and Roberts, R. G. (2008). Patterns of evolutionary conservation in the nesprin genes highlight probable functionally important protein domains and isoforms. *Biochem. Soc. Trans.* **36**, 1359-1367.

Starr, D. A. (2009). A nuclear-envelope bridge positions nuclei and moves chromosomes. *J. Cell Sci.* **122**, 577-586.

Starr, D. A. and Fischer, J. A. (2005). KASH 'n Karry: the KASH domain family of cargo-specific cytoskeletal adaptor proteins. *BioEssays* **27**, 1136-1146.

Stewart-Hutchinson, P. J., Hale, C. M., Wirtz, D. and Hodzic, D. (2008). Structural requirements for the assembly of LINC complexes and their function in cellular mechanical stiffness. *Exp. Cell Res.* **314**, 1892-1905.

Sullivan, T., Escalante-Alcalde, D., Bhatt, H., Anver, M., Bhat, N., Nagashima, K., Stewart, C. L. and Burke, B. (1999). Loss of A-type lamin expression compromises nuclear envelope integrity leading to muscular dystrophy. *J. Cell Biol.* **147**, 913-919.

Tzur, Y. B., Wilson, K. L. and Gruenbaum, Y. (2006). SUN-domain proteins: 'Velcro' that links the nucleoskeleton to the cytoskeleton. *Nat. Rev. Mol. Cell Biol.* **7**, 782-788.

Vaughan, A., Alvarez-Reyes, M., Bridger, J. M., Broers, J. L., Ramaekers, F. C., Wehnert, M., Morris, G. E., Whitfield, W. G. F. and Hutchison, C. J. (2001). Both emerin and lamin C depend on lamin A for localization at the nuclear envelope. *J. Cell Sci.* **114**, 2577-2590.

Wang, Q., Du, X., Cai, Z. and Greene, M. I. (2006). Characterization of the structures involved in localization of the SUN proteins to the nuclear envelope and the centrosome. *DNA Cell Biol.* **25**, 554-562.

Warren, D. T., Zhang, Q., Weissberg, P. L. and Shanahan, C. M. (2005). Nesprins: intracellular scaffolds that maintain cell architecture and coordinate cell function? *Expert Rev. Mol. Med.* **7**, 1-15.

Wheeler, M. A., Davies, J. D., Zhang, Q., Emerson, L. J., Hunt, J., Shanahan, C. M. and Ellis, J. A. (2007). Distinct functional domains in nesprin-1alpha and nesprin-2beta bind directly to emerin and both interactions are disrupted in X-linked Emery-Dreifuss muscular dystrophy. *Exp. Cell Res.* **313**, 2845-2857.

Wilhelmsen, K., Litjens, S. H., Kuikman, I., Tshimbalanga, N., Janssen, H., van den Bout, I., Raymond, K. and Sonnenberg, A. (2005). Nesprin-3, a novel outer nuclear membrane protein, associates with the cytoskeletal linker protein plectin. *J. Cell Biol.* **171**, 799-810.

Wilhelmsen, K., Ketema, M., Truong, H. and Sonnenberg, A. (2006). KASH-domain proteins in nuclear migration, anchorage and other processes. *J. Cell Sci.* **119**, 5021-5029.

Worman, H. J. and Courvalin, J.-C. (2004). How do mutations in lamins A and C cause disease? *J. Clin. Invest.* **113**, 349-351.

Worman, H. J. and Gundersen, G. G. (2006). Here come the SUNs: a nucleocytoskeletal missing link. *Trends Cell Biol.* **16**, 67-69.

Worman, H. J. and Bonne, G. (2007). "Laminopathies": a wide spectrum of human diseases. *Exp. Cell Res.* **313**, 2121-2133.

Ye, Q. and Worman, H. J. (1994). Primary structure analysis and lamin B and DNA binding of human LBR, an integral protein of the nuclear envelope inner membrane, *J. Biol. Chem.* **269**, 11306-11311.

Ye, Q., Callebaut, I., Pezhman, A., Courvalin, J.-C. and Worman, H. J. (1997). Domain-specific interactions of human HP1-type chromodomain proteins and inner nuclear membrane protein LBR. *J. Biol. Chem.* **272**, 14983-14989.

Zhang, Q., Skepper, J. N., Yang, F., Davies, J. D., Hegyi, L., Roberts, R. G., Weissberg, P. L., Ellis, J. A. and Shanahan, C. M. (2001). Nesprins: a novel family of spectrin-repeat-containing proteins that localize to the nuclear membrane in multiple tissues. *J. Cell Sci.* **114**, 4485-4498.

Zhang, Q., Ragnauth, C., Greener, M. J., Shanahan, C. M. and Roberts, R. G. (2002). The nesprins are giant actin-binding proteins, orthologous to Drosophila melanogaster muscle protein MSP-300. *Genomics* **80**, 473-481.

Zhang, Q., Ragnauth, C. D., Skepper, J. N., Worth, N. F., Warren, D. T., Roberts, R. G., Weissberg, P. L., Ellis, J. A. and Shanahan, C. M. (2005). Nesprin-2 is a multi-isomeric protein that binds lamin and emerin at the nuclear envelope and forms a subcellular network in skeletal muscle. *J. Cell Sci.* **118**, 673-687.

Zhang, Q., Bethmann, C., Worth, N. F., Davies, J. D., Wasner, C., Feuer, A., Ragnauth, C. D., Yi, Q., Mellad, J. A., Warren, D. T. et al. (2007a). Nesprin-1 and –2 are involved in the pathogenesis of Emery Dreifuss muscular dystrophy and are critical for nuclear envelope integrity. *Hum. Mol. Genet.* **16**, 2816-2833.

Zhang, X., Xu, R., Zhu, B., Yang, X., Ding, X., Duan, S., Xu, T., Zhuang, Y. and Han, M. (2007b). Syne-1 and Syne-2 play crucial roles in myonuclear anchorage and motor neuron innervation. *Development* **134**, 901-908.

Zhen, Y. Y., Libotte, T., Munck, M., Noegel, A. A. and Korenbaum, E. (2002). NUANCE, a giant protein connecting the nucleus and actin cytoskeleton. *J. Cell Sci.* **115**, 3207-3222.